Ultrasonics 67 (2016) 151–159

Contents lists available at ScienceDirect

Ultrasonics

journal homepage: www.elsevier.com/locate/ultras

Simulation study of a chaotic cavity transducer based virtual phased array used for focusing in the bulk of a solid material

Steven Delrue [a,*], Koen Van Den Abeele [a], Olivier Bou Matar [b]

[a] Wave Propagation and Signal Processing Research Group, KU Leuven Kulak, E. Sabbelaan 53, 8500 Kortrijk, Belgium
[b] Joint International Laboratory LICS/LEMAC: IEMN, UMR CNRS 8520, Univ. Nord de France, ECLille, Cité Scientifique, BP48, 59651 Villeneuve d'Ascq, France

ARTICLE INFO

Article history:
Received 27 August 2015
Received in revised form 15 January 2016
Accepted 18 January 2016
Available online 23 January 2016

Keywords:
Non-destructive testing
Time reversal
Chaotic cavity
Virtual phased array
Comsol

ABSTRACT

In acoustic and ultrasonic non-destructive testing techniques, it is sometimes beneficial to concentrate sound energy at a chosen location in space and at a specific instance in time, for example to improve the signal-to-noise ratio or activate the nonlinearity of damage features. Time Reversal (TR) techniques, taking advantage of the reversible character of the wave equation, are particularly suited to focus ultrasonic waves in time and space. The characteristics of the energy focusing in solid media using principles of time reversed acoustics are highly influenced by the nature and dimensions of the medium, the number of transducers and the length of the received signals. Usually, a large number of transducers enclosing the domain of interest is needed to improve the quality of the focusing. However, in the case of highly reverberant media, the number of transducers can be reduced to only one (single-channel TR). For focusing in a non-reverberant medium, which is impossible when using only one source, an adaptation of the single-channel reciprocal TR procedure has been recently suggested by means of a Chaotic Cavity Transducer (CCT), a single element transducer glued on a cavity of chaotic shape. In this paper, a CCT is used to focus elastic energy, at different times, in different points along a predefined line on the upper surface of a thick solid sample. Doing so, all focusing points can act as a virtual phased array transducer, allowing to focus in any point along the depth direction of the sample. This is impossible using conventional reciprocal TR, as you need to have access to all points in the bulk of the material for detecting signals to be used in the TR process. To asses and provide a better understanding of this concept, a numerical study has been developed, allowing to verify the basic concepts of the virtual phased array and to illustrate multi-component time reversal focusing in the bulk of a solid material.

© 2016 Elsevier B.V. All rights reserved.

1. Introduction

Time reversal (TR) techniques have become a vibrant topic of innovative research in ultrasonic applications [1–4]. The basic premise of time reversed acoustics (TRA) is that, if the wave field can be known as a function of time on some boundary surrounding a given region, then it can also be found at every point inside that region at previous times by using the wave equation with time running backwards. In other words, the result of a TR process is that the waves recorded on the boundary are focused back in space and time on the acoustic sources, or on the scattering targets inside the region which were acting as secondary sources. Doing so, it enables us to locate strong scatterers (e.g. inclusions and interfaces with high impedance contrast) which are hidden inside a region. Applications of TRA can be found in seismology (earthquake localization) [5–8], diagnostic and therapeutic medicine [9–12], and in non-destructive testing [13–20].

In a classical TRA experiment, waves generated by an acoustic source are first measured by an array of piezoelectric transducers located around the source, and then time reversed and re-emitted by the same transducers array. The created time reversed wave then propagates back and eventually focuses on the location of the initial source, now remaining passive. The quality of the focusing can be improved if the transducers cover a closed surface around the medium such that information is obtained from all wave fronts propagating in any possible direction [21]. In practice, however, this is difficult to realize and the TR operation is usually performed on a limited angular area, reducing the reversal focusing quality.

An important advantage of TRA for engineering materials is that it works extremely well in heterogeneous media (actually better

* Corresponding author. Tel.: +32 56246087; fax: +32 56246999.
E-mail addresses: Steven.Delrue@kuleuven-kulak.be (S. Delrue), Koen.VanDenAbeele@kuleuven-kulak.be (K. Van Den Abeele), olivier.boumatar@iemn.univ-lille1.fr (O. Bou Matar).

http://dx.doi.org/10.1016/j.ultras.2016.01.010
0041-624X/© 2016 Elsevier B.V. All rights reserved.

than in homogeneous ones). Multiple scattering in transmission experiments [22] or multiple reflections in wave guides [23–26] or inside chaotic cavities [27–29], instead of being a hindrance, actually improve the focusing. This reduces the number of receivers needed to obtain a good reversal quality. Draeger et al. [27–29] and Fink et al. [30] even proved the possibility of reducing the number of elements down to one by using multiple reflections inside a closed chaotic cavity. In addition, it was shown that the focusing quality can be increased by a longer recording of the time reversed signal [27]. However, for too long time windows, the focusing quality can no more be improved, since the essential signal information can no longer be discerned from noise due to attenuation in the material.

In standard single-channel TR experiments, a signal measured by the receiver is time reversed and subsequently re-emitted back into the medium by a transducer located at the same position as the receiver, resulting in a focusing at the original source position [8]. Due to reciprocity in acoustic and elastic wave propagation, the back propagation of the time reversed signal from the position of the original source to the position of the corresponding receiver will result in a focus of energy at the actual receiver location [31]. This procedure is called reciprocal TR. Implementation of reciprocal TR thus allows to selectively focus acoustic/elastic energy at any position in a given medium, provided the direct received signal can be predicted or obtained at that position, for instance by an appropriate material model or – for surface locations – by recording the signal using a laser vibrometer or a non-contact transducer. In a number of studies, the reciprocal TR technique has been used to focus a large amount of energy at a certain position in order to trigger nonlinear features at that location [14,15,32].

In case of a non-reverberant sample, the above described TR technique cannot be used anymore, since the absence of reflections implies that the only information path between the source and the receiver is the direct path. For an accurate re-focusing of the energy multiple information paths coming from different directions (i.e. originating at different virtual source locations) are required. Recently, a solution for this problem was proposed using a Chaotic Cavity Transducer (CCT), consisting of a transducer glued to a cavity of chaotic shape, which itself is placed in or connected to a non-reverberant medium. The principle of a CCT was originally introduced for 3D imaging in fluids [33–37] and was later extended to applications dealing with elastic waves in solids. Van Damme et al. [38] experimentally investigated the use of a CCT for elastic imaging in reverberant and non-reverberant solid media. Choi et al. [39] described the construction of a CCT based 2D virtual array used for pulse-echo type non-destructive inspection of solid materials. In this paper, we also discuss a CCT based virtual array using a finite element based model developed in the commercially available software package Comsol Multiphysics. However, other than the ultrasonic 3D imaging described by Choi et al., we will use the virtual phased array to focus elastic energy at a predefined location in the bulk of a solid material. This is of great importance, as such a TR focusing cannot be obtained using conventional reciprocal TR since we do not have access to points in the bulk of the material to detect the signals to be used in the TR process. Virtual experiments will be performed, verifying and illustrating this innovative concept. In future, the numerical model can be modified and extended to help in the further development and optimization of linear and nonlinear imaging techniques based on TR principles.

2. Time reversal modeling approach

To demonstrate the feasibility and usefulness of single-channel reciprocal TR techniques using a chaotic cavity transducer, we exploit a fully numerical approach that covers the emission of a virtual sound wave from the source location, the recording of the forward wave propagation signal (single or multiple components) at a particular receiver position, the back propagation of the time reversed signal(s) from the original location of the emitter and the analysis of the energy focusing quality at the considered receiver location. In traditional TR experiments, the source signal consists of a short pulse, which is applied to the transducer. To obtain spatial and temporal focusing, the impulse response of this signal, measured by the receiver, is time reversed and broadcasted back into the medium. It is shown, however, that the quality of the focusing can be improved by (1) applying a pulse compression technique, which involves the use of a linear sweep signal (also known as chirp) as excitation signal instead of a short pulse [38,40–42] and (2) by utilizing a deconvolution, or inverse filtering, technique [43]. In the present simulations, a combination of both is used. Since the simulations represent wave propagation phenomena in a supposedly linear medium, the finite element model used for the TR simulations is solved in frequency domain. Moreover, taking advantage of the spectral method, one can obtain the exact same solution of the model without performing two separate simulations (i.e. one for the forward propagation and one for the back propagation phase).

The model is first solved for a discrete number of frequencies using a constant amplitude equal to one as an input for the boundary condition at the source. This input actually corresponds to the Fourier Transform (FFT) of an impulse. For every frequency, the complex valued amplitudes calculated in each point of the model are then stored. These stored solutions are corresponding to the impulse responses, or the Green functions $G_i(\omega)$, at each position, where index i denotes a particular position. The complex valued signals $R_i(\omega)$, recorded in response to a linear swept signal $S(\omega)$ (or rather from the FFT of $S(t)$), can then be calculated as follows:

$$R_i(\omega) = G_i(\omega) \cdot S(\omega).$$

For the back propagation of a particular recorded signal $R_j(\omega)$ $(i = j)$, we first apply pulse compression by performing a point-wise multiplication of the complex conjugate of the linear swept signal $S(\omega)$ and the recorded signal $R_j(\omega)$. Subsequently, inverse filtering is applied by dividing the obtained signal by the square of the norm of $R_j(\omega)$ (i.e. $|R_j(\omega)|^2$). As such, we get the following transformation:

$$R_j(\omega) \rightarrow \frac{R_j(\omega) \cdot S^*(\omega)}{|R_j(\omega)|^2 + \epsilon_j},$$

where $*$ denotes the complex conjugate operation and ϵ_j is a constant added to the denominator to ensure that we never divide by zero. The constant is related to the original received signal as follows [43]:

$$\epsilon_j = 0.9 \text{ mean}(|R_j(\omega)|^2).$$

Finally, the focusing signals $F_i(\omega)$ are calculated by multiplying – frequency by frequency – the Green functions $G_i(\omega)$ by the complex conjugate of the obtained signal (i.e. the FFT of the time reversed signal after pulse compression and inverse filtering):

$$F_i(\omega) = G_i(\omega) \cdot \left(\frac{R_j(\omega) \cdot S^*(\omega)}{|R_j(\omega)|^2 + \epsilon_j} \right)^*. \quad (1)$$

One can easily see, that for $i = j$ (i.e. the position where the direct received signal was obtained), the focusing signal becomes:

$$F_j(\omega) = \frac{|R_j(\omega)|^2}{|R_j(\omega)|^2 + \epsilon_j} \approx 1,$$

which approximates the spectrum of a delta function $\delta(t)$.

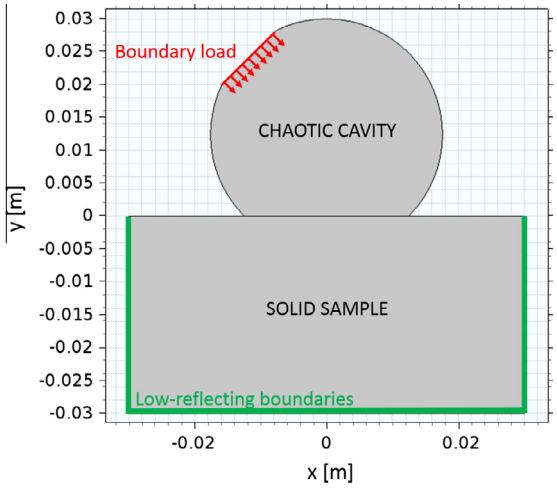

Fig. 1. Illustration of the geometry of a chaotic cavity transducer on top of a large solid sample used in the Comsol simulation. The chaotic cavity transducer has a maximum height of 3 cm and a maximum width of 3.5 cm. The solid sample has a height of 3 cm and a width of 6 cm and is modeled using low-reflecting boundaries.

The application of single-channel reciprocal TR allows not only to focus in one point, but also in multiple points (simultaneously or with a well defined delay). This is done by using the algebraic sum of the (time delayed) signals recorded in the different points as a new input in the TR process. As such, Eq. (1) to calculate the focusing signals $F_i(\omega)$ is changed as follows:

$$F_i(\omega) = G_i(\omega) \cdot \sum_{j=1}^{N} \left(\frac{R_j(\omega) \cdot S^*(\omega)}{|R_j(\omega)|^2 + \epsilon_j} \right)^*, \tag{2}$$

where N is the number of focal positions and

$$R_j(\omega) = G_j(\omega) \cdot S(\omega) \cdot \exp(-i\omega\Delta t_j)$$

to take into account the desired time delays Δt_j.

Note that in every step of the simulation, the time domain signals can be obtained by performing an inverse FFT of the data. Using this spectral method, the TR simulations become less time consuming. Moreover, if there are no changes in the geometry, the solutions for different parameters (e.g. different source signals, different focal points, etc.) can be determined using only the stored data $G_i(\omega)$ from one simulation.

3. CCT based time reversal

For the actual implementation of CCT based reciprocal time reversal, we consider a 2D simulation model consisting of an aluminum chaotic cavity glued to the upper surface of a long (x-direction) and thick (y-direction) solid sample, modeled as a finite size rectangular medium with low-reflecting boundaries, mimicking the large sample size (see Fig. 1). The cavity has a circular shape with two flat sides. The longest of the flat sides is attached to the sample (perfect bonding is assumed), the shortest flat side accommodates a source (infinitesimal thin and flat transducer) and is considered to be the active surface of the chaotic cavity. The maximum height of the cavity is 3 cm and the maximum width is 3.5 cm. All boundaries of the cavity, except for the active surface of the chaotic cavity and the flat side connected to the sample, are expected to be free boundaries. At the source location (transmitter), a normal boundary load with constant amplitude equal to one was added, as described in Section 2. At the interface between the cavity and the sample, continuity has been assumed. The density of the solid sample is considered to be equal to 1000 kg/m^3 and the longitudinal and shear velocities are respectively 3000 m/s and 1500 m/s. The density of the chaotic cavity was set equal to 2700 kg/m^3 and the longitudinal and shear velocity are respectively 6320 m/s and 3130 m/s. In the numerical experiments, a single or multiple receiver locations can be considered anywhere in the reverberant sample.

To demonstrate the single-channel reciprocal TR method, we model the following numerical experiment. First, a linear swept signal is generated at the active surface of the transmitter (i.e. the flat side at the top of the chaotic cavity). The signal is defined as follows:

$$S(t) = \sin\left(2\pi f_0 t + \frac{\pi B t^2}{T}\right) \exp\left[-\frac{1}{p}\left(\frac{t - t_c}{\sigma}\right)^p\right]$$

with start frequency $f_0 = 300$ kHz, bandwidth $B = 600$ kHz and duration $T = 100$ μs. In order to reduce time domain side lobes which may appear in the pulse compression process, the swept signal was multiplied with a generalized Gaussian time window with exponent $p = 20$, central time $t_c = T/2$ and standard deviation σ, chosen such that the amplitude of the Gaussian envelope at times $t = 0$ and $t = T$ equals one percent of the amplitude at time $t = t_c$. When the emitted signal reaches the interface between the cavity and the solid sample, part of the signal is reflected and keeps propagating in the cavity, while an other part is transmitted into the sample. This process keeps going on till no more energy is trapped in the cavity. During the process, part of the transmitted energy enters the solid sample with irregular time delays, and propagates in different directions towards the supposed receiver location(s). The signal at the receiver location (or at multiple receiver locations) is then recorded and, after performing pulse compression and inverse filtering, used as a new input signal in the back propagation step of the TR process. Finally, the zone around the receiver location (s) is analyzed to validate the evidence of TR focusing both in time and space. It is important to note that this TR focusing is fully caused by the reflections inside the chaotic cavity. The non-reverberant medium itself is not responsible for the focusing due to a lack of reflections.

3.1. Direct time reversal method

Using single-channel reciprocal TR in combination with a chaotic cavity, we are able to focus energy at any position in a non-reverberant medium. Moreover, we are able to selectively focus energy in a specific displacement component [44]. This is demonstrated in Fig. 2, where the horizontal displacement component u_x at the focal position $(0, -2)$ cm (encircled in the figures, inside the solid sample) was used as an input signal (normal to the surface) in the back propagation step of the reciprocal TR. This results in a selectively TR focusing in time and space only along the horizontal displacement component. Fig. 2(a) displays the simulated time signals of both displacement components at the focal position (illustrating the focusing in time) and Fig. 2(b) shows the respective spatial distribution of the magnitude of the displacement components at the focal time (illustrating the focusing in space). Similar results can be obtained for focusing along the vertical displacement component u_y.

3.2. Virtual phased array time reversal method

As discussed in Section 2 (Eq. (2)), we can also apply the chaotic cavity transducer TR focusing procedure to focus elastic energy (simultaneously or with a well defined delay Δt_j) in multiple points inside the solid sample. Using this result and the principle of Huygens, we can then use the chaotic cavity transducer to create a virtual phased array, enabling the focusing of energy in any arbitrary

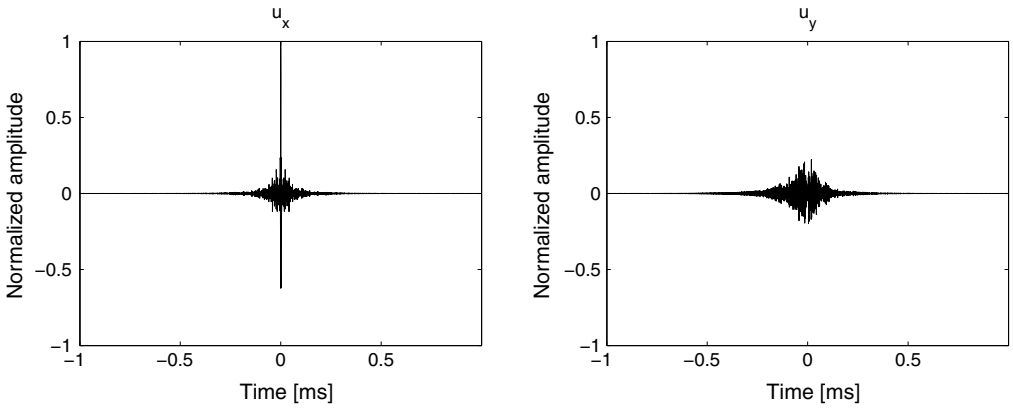

(a) Illustration of focusing in time

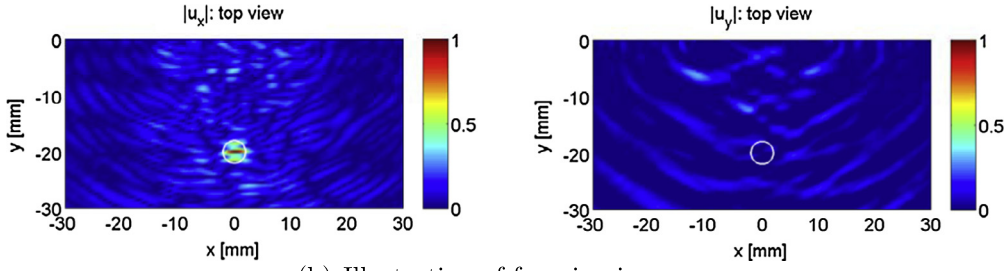

(b) Illustration of focusing in space

Fig. 2. Simulated displacements in a large solid sample after reciprocal TR of the direct recorded horizontal displacement component u_x. The focal position is located at $(0,-2)$ cm and is encircled in the bottom figures. (a) Simulated horizontal and vertical displacement signals u_x and u_y measured at the focal position, (b) spatial (top view) surface plots of the magnitude of the horizontal and vertical displacement components u_x and u_y at the focal time. The color scales are normalized according to the maximum value of the horizontal displacement component. (For interpretation of the references to colour in this figure legend, the reader is referred to the web version of this article.)

position in the bulk of both reverberant and non-reverberant media. Phased array probes are composed of multiple ultrasonic elements that can transmit waves independently at different times. They can be used to focus ultrasonic beams, applying time delays to the elements to create constructive interference of the wave fronts, allowing the energy to be focused at any position in the medium.

In order to transform a chaotic cavity transducer into a phased array, a well-defined sequence of preparatory steps needs to be followed. As in the previous examples, we start with the excitation of a linear swept signal. Subsequently, the response signals are measured in a series of points located on a line at the interface between the cavity and the sample. Then, a specific combination of these direct recorded signals is formed and used in the TR process according to Eq. (2), where time delays Δt_j are depending on the location of the desired focal point. In case all time delays equal zero, the TR process will result in a simultaneous focusing of energy in all considered recording positions. At that particular focusing instance, every "recording" point may be considered as a source of secondary wavelets that spread out in all directions. In case of the simultaneous energy focusing, a plane wave is created propagating in the direction perpendicular to the recording line. However, when relative time delays are introduced before summing the signals, the focal time in every point will be different. Consequently, the "recording" points radiate secondary waves at different times. Thus, choosing and applying appropriate time delays we should be able to focus energy in an arbitrary point in the bulk of a solid sample. The required time delays can be calculated by determining the distances between the recording points and the intended focal point and dividing these distances by the wave propagation speed in the considered medium. The direct recorded signals are then time shifted such that the energy is first focused in the recording points furthest away from the intended focal point, and last in the recording points which are closest to that point.

To successfully create a virtual phased array in a medium, the wave speed distribution in the medium needs to be known in order to determine the appropriate time delays of the different recording signals. For a chaotic cavity connected to a fluid, the technique works very well, since waves can only propagate with the longitudinal wave velocity [35–37]. In a solid material, however, the focusing using a virtual phased array becomes less straightforward, since waves can propagate inside the material either with the longitudinal wave velocity or with the transversal wave velocity. Moreover, in semi-infinite half-spaces and in plates, the presence of Rayleigh and Lamb waves even can play an important role. And finally, anisotropy and heterogeneity can make the picture even more complicated.

To obtain a better understanding of the concept of the virtual phased array in solids, we repeat the study of the 2D configuration of an aluminum chaotic cavity connected to the upper surface of a large solid sample, as illustrated in Fig. 1. This time, after emitting a sweep signal (i.e. the same sweep signal used before), the response signals (i.e. horizontal or vertical displacement components) are measured in 49 recording points located at the interface between the cavity and the solid material (i.e. $y=0$) and with x-coordinates starting from -1.2 cm to 1.2 cm in steps of 0.5 mm. The recording points serve as the emitter positions of the virtual phased array. Our goal is to successfully focus energy along the spatial directions at an arbitrary point in the bulk of the solid sample using the virtual phased array concept.

Before focusing at an arbitrary point in the medium using appropriate time delays, we first study the generation of plane waves created by simultaneously focusing the energy selectively

along the horizontal or vertical displacement component in all 49 recording points. In the first simulation, we re-emitted the sum signal of the direct recorded horizontal displacement components at the recording positions, resulting in a simultaneous focusing of energy along the horizontal displacement component in all recording points. This is illustrated in Fig. 3, where spatial maps of the magnitude of the horizontal displacement component inside the solid material are shown at three subsequent times ($t = 4$ μs, $t = 8$ μs and $t = 12$ μs). We clearly observe the propagation of a plane wave (indicated by an arrow) that was created by simultaneous TR focusing in the recording points at the time corresponding to the "line focusing time" (i.e. $t = 0$). The simultaneous focusing of the horizontal component will create secondary waves from horizontally oriented dipoles with energy propagating with both the longitudinal and transversal wave velocity. The part of the wave traveling at the longitudinal wave velocity will mainly propagate in the horizontal direction, while the part traveling at the transversal wave velocity will primarily propagate in the vertical direction. Since the only constructive interference will occur in the vertical propagation direction, a plane wave will be created preferentially propagating with the transversal wave velocity in the direction normal to the recording line. This is verified by noting that the plane wave amplitude peak observed in Fig. 3 takes 12 μs to travel a distance of 1.8 cm from the recording points at $y = 0$ mm to $y = -18$ mm. Dividing this distance by the travel time, we indeed find the shear velocity ($v_T = 1500$ m/s).

A similar study can be performed for a simultaneous TR focusing of the vertical displacement component in all 49 recording points. However, in this case, the simultaneous focusing of the vertical component will create secondary waves from vertically oriented dipoles with the part that travels at the longitudinal wave velocity mainly propagating in the vertical direction and the part traveling at the transversal wave velocity mainly propagating in the horizontal direction. Consequently, the created plane wave will preferentially propagate with the longitudinal wave velocity ($v_L = 3000$ m/s) in the direction normal to the recording line.

From the above discussed results, it follows that TR focusing of the horizontal (vertical) displacement components in the recording points results in the creation of secondary waves, originating at the recording points and generating a plane wave propagating perpendicularly to the recording line with the transversal (longitudinal) velocity. With this knowledge, we are now able to calculate the proper time delays of the different recording signals, in order to selectively focus along each spatial direction at an arbitrary point in the bulk of the medium using the virtual phased array.

To focus the horizontal displacement component at an arbitrary position, we first need to focus the horizontal displacement components at the recording positions, with appropriate time delays. Since this focusing will create secondary waves (from horizontally oriented dipoles) preferentially propagating with the transversal wave velocity in the direction perpendicular to the recording line, the time delays can be calculated by determining the distance of the recording points to the intended focal point divided by this velocity. For a focal point located at $(0, -2)$ cm inside the solid material, the calculations reveal that, in order to focus the horizontal displacement component at the focal time $t = 0$ in point $(0, -2)$ cm, the focusing in the recording points needs to be 12 μs (for the middle recording position) to 14.4 μs (for the left- and rightmost recording positions) earlier, i.e., a time difference of 1.44 periods in the case of a central frequency of 600 kHz. The non-simultaneous TR focusing in the recording points creates a curved wave front propagating in the negative y-direction. Finally, at $t = 0$, the secondary waves radiated by the virtual phased array positions constructively interfere with each other, resulting in a clear TR focusing at the intended focal position. Fig. 4 confirms that the focusing only occurs in the horizontal displacement component. Fig. 4(a) represents the simulated time signals for both displacement components at the focal position. Fig. 4(b) represents spatial maps of the magnitude of respectively the horizontal and vertical displacement fields at the focal time. TR focusing in time and space is only observable in the horizontal displacement component.

A similar procedure can be applied to focus the vertical displacement component at $(0, -2)$ cm inside the non-reverberant material. In this case, we first focus the vertical displacement components, with appropriate time shifts, at the 49 recording positions. This will create secondary waves (dipoles with energy in

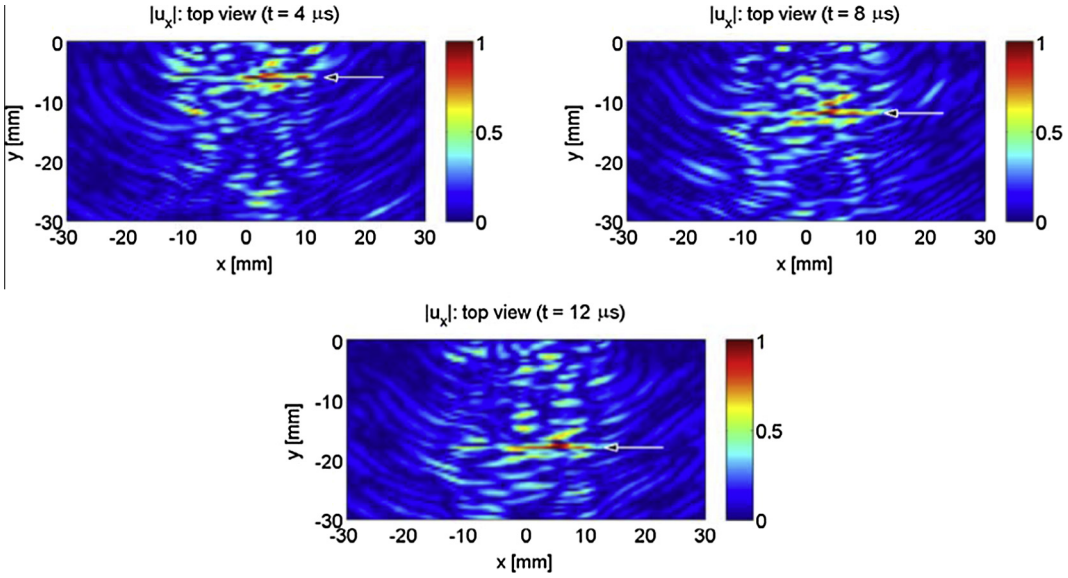

Fig. 3. Top view surface plots of the simulated magnitude of the horizontal displacement component in a large solid sample after reciprocal TR of the sum of the direct recorded horizontal displacement components u_x in 49 recording points. The results are plotted for three different times: $t = 4$ μs, $t = 8$ μs and $t = 12$ μs. The arrow marks the average position of the plane wave front that was created by simultaneous TR focusing in the recording points. The color scales are normalized according to the maximum value of the horizontal displacement component in each time step. (For interpretation of the references to colour in this figure legend, the reader is referred to the web version of this article.)

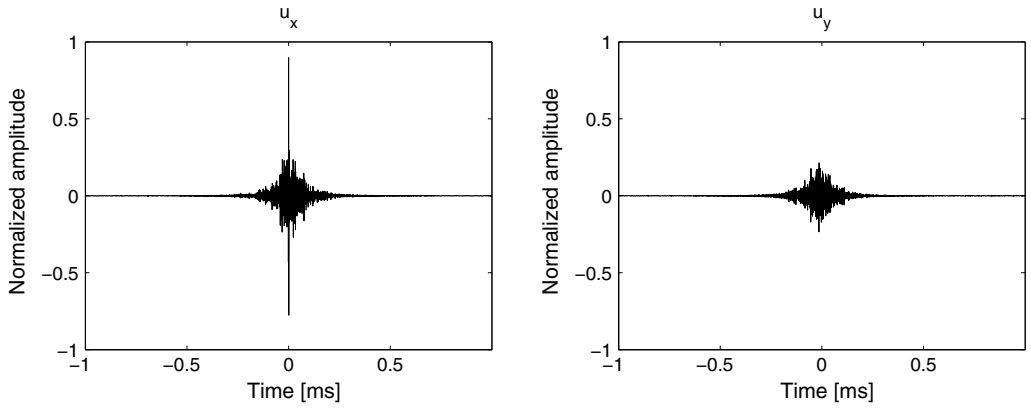

(a) Illustration of focusing in time

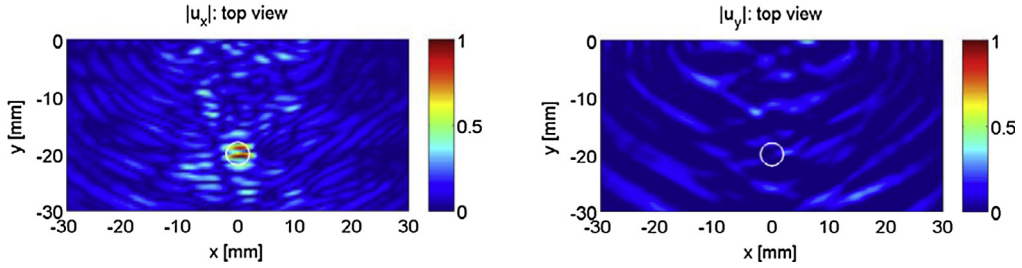

(b) Illustration of focusing in space

Fig. 4. Simulated displacements in a large solid sample after reciprocal TR of the direct recorded horizontal displacement component u_x using a virtual phased array. The focal position is located at $(0,-2)$ cm and is encircled in the bottom figures. (a) Simulated horizontal and vertical displacement signals u_x and u_y measured at the focal position, (b) spatial (top view) surface plots of the magnitude of the horizontal and vertical displacement components u_x and u_y at the focal time. The color scales are normalized according to the maximum value of the horizontal displacement component. (For interpretation of the references to colour in this figure legend, the reader is referred to the web version of this article.)

the vertical direction) preferentially propagating at the longitudinal wave velocity. The time delays should therefore be calculated using the distance of the recording points to the focal point divided by the longitudinal wave velocity. The calculated time shifts reveal that the TR focusing in the recording points needs to be 6 μs (for the middle recording position) to approximately 7 μs (for the left- and rightmost recording positions) earlier than the focusing in the focal point at $t=0$. Due to the appropriate time delays, a curved wave front is created that propagates in the negative y-direction until it finally focuses at the intended focal point at $t=0$. In this case, focusing is only observed for the vertical displacement component, as confirmed by Fig. 5. Fig. 5(a) represents the time signals of respectively the simulated horizontal and vertical displacements at the focal point, showing a clear focusing in time only in the y-component of the displacement. Fig. 5(b) represents spatial maps of the magnitude of the horizontal and vertical displacement in the sample at the focal time, illustrating the focusing in space of the y-component of the displacement.

The use of a virtual phased array has a great advantage over the direct TR method. To focus energy at an arbitrary point (x_1,y_1) inside a medium using the direct TR method, the direct response signal needs to be known at that point inside the medium. For a focusing at (x_2,y_2) one needs again the direct response at that point, etc. A full scan of a zone of the medium using direct TR focusing thus requires to know the direct response signals at any point within the zone of interest, which is often not possible. With the virtual phased array, however, only the response signals in a limited number of recording points are required (these points can even be outside the zone of interest). Changing the time shifts of the different recording signals we are able to focus in any point of a predetermined inspection zone. Results of this procedure are illustrated in Fig. 6. Using the same virtual array recording positions as before (i.e. 49 positions located at the interface of the cavity and the solid sample, with x-coordinates ranging from $x=-1.2$ cm to $x=1.2$ cm), the time shifts necessary to focus respectively the horizontal and vertical displacement component in any point in the bulk of the solid sample are calculated. Fig. 6 (a) represents a spatial map of the quality of the temporal focusing in the horizontal displacement component u_x, whereas Fig. 6(b) represents the quality of the temporal focusing in the vertical displacement component u_y. The quality $Q(x,y)$ of the temporal focus at position (x,y) was calculated as follows:

$$Q(x,y)=\frac{\max_t[u_i(x,y,t)^2]}{\mathrm{mean}_t[u_i(x,y,t)^2]}, \tag{3}$$

where $u_i(x,y,t)$ is the displacement of point (x,y) at time t ($i\in\{x,y\}$). The quality at position (x,y) is thus equal to the ratio of the maximum, over all times t, of the squared displacement amplitudes to the mean, over all times t, of the squared displacement amplitudes. From the figures it is clear that high quality focusing in both displacement components is obtained at positions right under the virtual phased array, in a region which is diverging with decreasing y-coordinate. Variations in the quality obtained within that region are supposed to be due to the shape of the chaotic cavity, however, this still needs to be investigated in future. Outside the diverging region, the focusing quality deteriorates. The diverging region for high quality focusing in the horizontal displacement component u_x is much smaller than the region for high quality focusing in the vertical displacement component u_y. This is explained as follows. In case of simultaneous focusing in the recording points (cfr. Fig. 3), the virtual phased array produces an ultra-

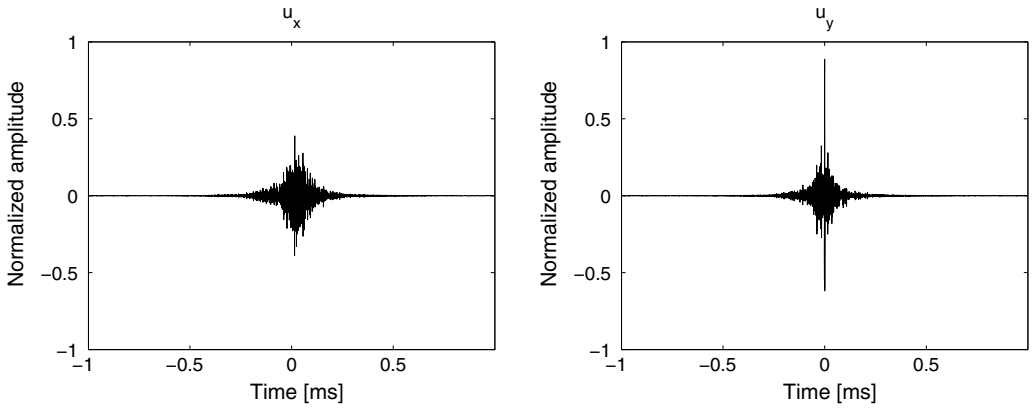

(a) Illustration of focusing in time

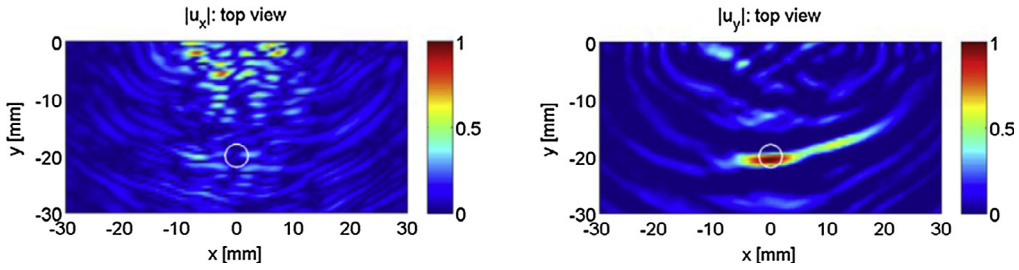

(b) Illustration of focusing in space

Fig. 5. Simulated displacements in a large solid sample after reciprocal TR of the direct recorded vertical displacement component u_y using a virtual phased array. The focal position is located at $(0,-2)$ cm and is encircled in the bottom figures. (a) Simulated horizontal and vertical displacement signals u_x and u_y measured at the focal position, (b) spatial (top view) surface plots of the magnitude of the horizontal and vertical displacement components u_x and u_y at the focal time. The color scales are normalized according to the maximum value of the horizontal displacement component. (For interpretation of the references to colour in this figure legend, the reader is referred to the web version of this article.)

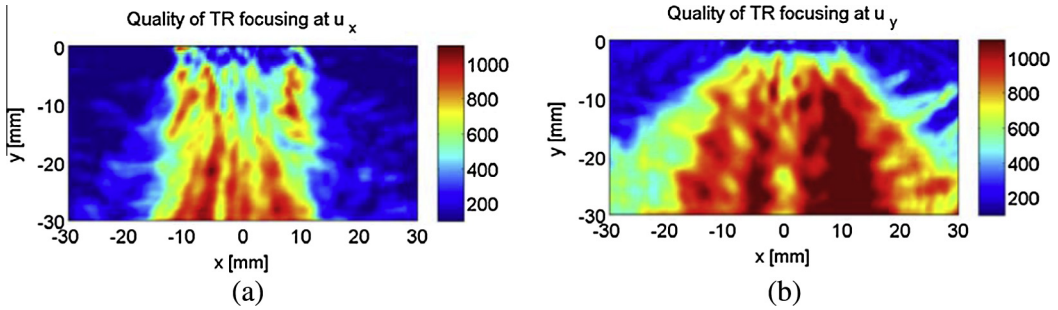

Fig. 6. Spatial (top view) surface plots of the quality of the temporal TR focusing in any point along the depth direction of a large solid sample using a virtual phased array. The quality was measured according to formula (3). (a) Quality of the temporal TR focusing in the horizontal displacement component u_x, (b) quality of the temporal TR focusing in the vertical displacement component u_y.

sonic wave that has properties similar to the properties of a single transducer with an effective width corresponding to the virtual phased array aperture (i.e. 2.4 cm). Therefore, the produced ultrasonic wave is diverging with an angle inversely proportional to the transducer diameter and proportional to the wavelength of the transmitted sound wave. In case of focusing in the horizontal displacement component at the recording points, a plane shear wave is created of which the wavelength is smaller than the wavelength of the longitudinal plane wave that is created when focusing in the vertical displacement components. Consequently, the divergence angle of the generated plane shear wave is smaller than that of the generated plane longitudinal wave. When the virtual phased array is used for focusing, the produced ultrasonic wave is steered in any direction, with the maximum steering angle being limited by the above mentioned divergence angles. As such, we obtain a larger steering angle for focusing in the vertical displacement component when compared to the angle obtained for focusing in the horizontal displacement component.

The above discussed numerical results illustrate the possibility to focus elastic energy along the depth of a material, using a CCT based virtual phased array at the interface of the chaotic cavity and the sample. However, to implement this concept in practice, we need to have access to all points along the line of the phased array for detecting the signals to be used in the time reversal process. This, of course, is not possible when the cavity is already connected to the sample. Therefore, we checked the possibility to perform the calibration step before the cavity is being glued to the solid sample. For this, the following steps need to be followed. We start with exciting the chaotic cavity using the same linear swept signal that we used before. Subsequently, the response sig-

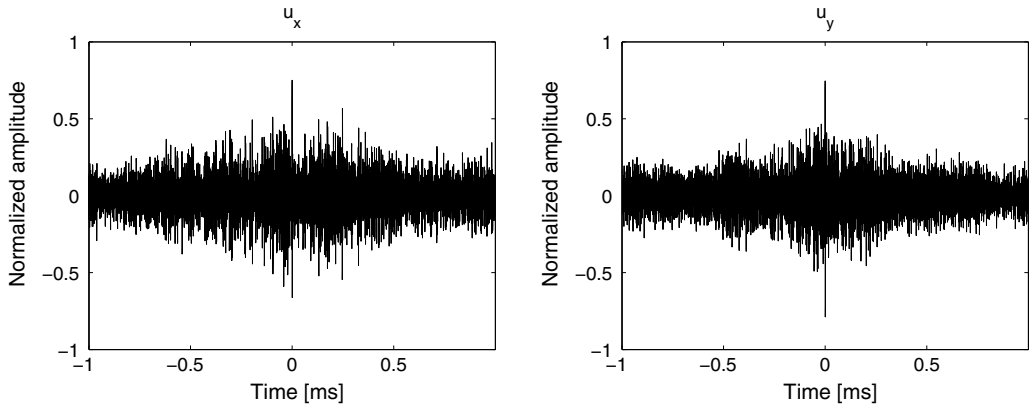

(a) Illustration of focusing in time

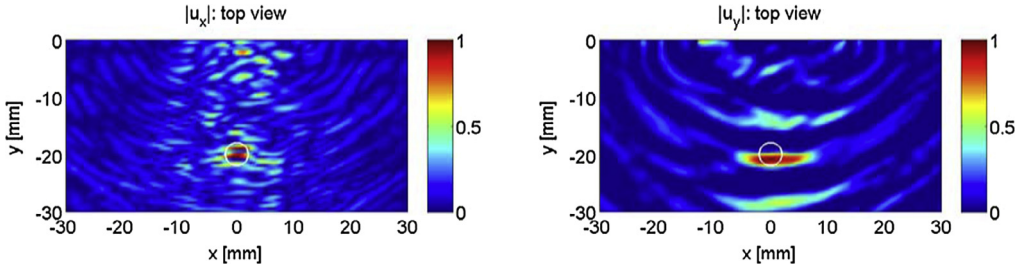

(b) Illustration of focusing in space

Fig. 7. Simulated displacements in a large solid sample after reciprocal TR of either the direct recorded horizontal displacement component u_x or the vertical displacement component u_y using a virtual phased array. The recorded signals were measured at the bottom surface of the chaotic cavity before the cavity was glued to the sample. The focal position is located at $(0, -2)$ cm and is encircled in the bottom figures. (a) Simulated displacement signals at the focal position after re-emission of respectively the direct recorded horizontal and vertical displacement signals u_x and u_y, (b) spatial maps of the magnitude of both displacement components at the focal time after re-emission of respectively the direct recorded horizontal and vertical displacement signals u_x and u_y. The color scales are normalized according to the maximum value of the horizontal displacement component. (For interpretation of the references to colour in this figure legend, the reader is referred to the web version of this article.)

nals are measured in a series of points located on a line at the bottom surface of the cavity. Then, the cavity is glued to the solid sample and a specific combination of the recorded signals (depending on the location of the desired focal position) is re-emitted into the cavity in order to focus in any position in the bulk of the solid sample. Fig. 7 confirms that, using this approach, TR focusing in respectively the horizontal and vertical displacement component at position $(0, -2)$ cm inside the sample is still observable, be it with a higher noise level as when compared to respectively the left figures from Fig. 4 and the right figures from Fig. 5. The drop in focusing quality is caused by the change in the recorded signals due to a difference in loading between the calibration step and when the chaotic cavity is loaded with the solid sample. Another solution on how to practically get the direct signals in an actual experiment can be to add a (relatively thin) patch-type receiving transducer in between the chaotic cavity and the solid sample, similar to what was described by Choi et al. [39]. The direct signals can then be recorded by the receiving patch before they are re-emitted into the chaotic cavity.

4. Conclusions

The principle of a chaotic cavity transducer was originally introduced for 3D imaging in fluids and was later extended to applications dealing with elastic waves in solids, for instance for constructing a 2D virtual array used for pulse-echo type non-destructive inspection of materials. In this paper, we have provided numerical supporting evidence of a new application of the chaotic cavity based virtual phased array: the ability of time reversal focusing of elastic energy in the bulk of a large solid material. Using the developed finite element model, we were able to verify the basic concepts of the virtual phased array and illustrated multi-component TR in any point along the depth direction of a large solid sample. In the considered 2D configuration, it was shown that TR focusing along the horizontal displacement component could be achieved if the transversal wave velocity was used to determine the proper time shifts, while the longitudinal wave velocity needs to be used for TR focusing along the vertical displacement component.

Future work will consist in studying the influence of the impedance mismatch between the chaotic cavity and the solid sample on the TR focusing quality. We expect limitation in implementing the procedure for large and small impedance mismatch. In case of a large impedance mismatch, the signals will only propagate in the cavity without being transmitted to the solid, while in case of a small impedance mismatch all signals will be transmitted and no internal reflections (crucial for TR purposes) will occur in the cavity itself. We also plan to study the influence of the shape of the chaotic cavity on the focusing quality. Apart from the presented 2D configuration, we also want to proceed to more complex 3D configurations. A suitable technique to determine the wave speed distribution inside materials needs to be developed, especially in the case of anisotropic materials. Another interesting problem would be to study the behavior of a chaotic cavity transducer embedded in a solid material. Industrial components designed with such embedded chaotic cavity transducers could then be used as self-sensing devices, with obvious applications in aeronautics, automotive, construction engineering, etc. The ultimate goal of the simulations is to optimize the technique for such practical uses.

Acknowledgments

This work is supported by the Research Council of the Katholieke Universiteit Leuven (OT/07/051, CIF1), and by the Flemish Fund for Scientific Research (G.0554.06, G.0443.07)

References

[1] M. Fink, Time reversal of ultrasonic fields – part 1: basic principles, IEEE Trans. Ultrason. Ferroelectr. 39 (1992) 555–566.
[2] M. Fink, Time reversed acoustics, Phys. Today 50 (1997) 34–40.
[3] M. Fink, Time-reversed acoustics, Sci. Am. 281 (1999) 91–97.
[4] M. Fink, D. Cassereau, A. Derode, C. Prada, P. Roux, M. Tanter, J. Thomas, F. Wu, Time-reversed acoustics, Rep. Prog. Phys. 63 (2000) 1933–1995.
[5] C. Larmat, R. Guyer, P. Johnson, Time-reversal methods in geophysics, Phys. Today 63 (2010) 31–35.
[6] C. Larmat, J. Tromp, Q. Liu, J. Montagner, Time reversal location of glacial earthquakes, J. Geophys. Res. – Solid Earth 113 (2008) B09314.
[7] C. Larmat, J. Montagner, M. Fink, Y. Capdeville, A. Tourin, E. Clevede, Time-reversal imaging of seismic sources and application to the great Sumatra earthquakes, Geophys. Res. Lett. 33 (2006) 1–4.
[8] B. Anderson, M. Griffa, C. Larmat, T. Ulrich, P. Johnson, Time reversal, Acoust. Today 4 (2008) 5–16.
[9] M. Fink, G. Montaldo, M. Tanter, Time-reversal acoustics in biomedical engineering, Annu. Rev. Biomed. Eng. 5 (2003) 465–497.
[10] H. Trefna, J. Vrba, M. Persson, Time-reversal focusing in microwave hyperthermia for deep-seated tumors, Phys. Med. Biol. 55 (2010) 2167–2185.
[11] M. Porter, P. Roux, H. Song, W. Kuperman, Tumor treatment by time-reversal acoustics, in: Acoustics, Speech, and Signal Processing, Proceedings, Vol. 4, Phoenix, 1999, pp. 2107–2110.
[12] S. Dos Santos, M. Domenjoud, Z. Prevorsky, Ultrasonic imaging of human tooth using chirp-coded nonlinear time reversal acoustics, Phys. Proc. 3 (2010) 913–918.
[13] E. Saenger, G. Kocur, R. Jud, M. Torrilhon, Application of time reverse modeling on ultrasonic non-destructive testing of concrete, Appl. Math. Model. 35 (2011) 807–816.
[14] T. Ulrich, A. Sutin, R. Guyer, P. Johnson, Time reversal and non-linear elastic wave spectroscopy (TR NEWS) techniques, Int. J. Nonlinear Mech. 43 (2008) 209–216.
[15] T. Ulrich, A. Sutin, T. Claytor, P. Papin, P. Le Bas, J. TenCate, The time reversed elastic nonlinearity diagnostic applied to evaluation of diffusion bonds, Appl. Phys. Lett. 93 (2008) 151914.
[16] T. Goursolle, S. Dos Santos, O. Bou Matar, S. Callé, Non-linear based time reversal acoustic applied to crack detection: simulations and experiments, Int. J. Nonlinear Mech. 43 (2008) 170–177.
[17] A. Sutin, P. Johnson, J. TenCate, Development of nonlinear time reversed acoustics (NLTRA) for applications to crack detection in solids, in: Proceedings of the World Congress on Ultrasonics, Paris, 2003, pp. 155–158.
[18] A. Sutin, P. Johnson, Nonlinear elastic wave NDE II: nonlinear wave modulation spectroscopy and nonlinear time reversed acoustics, Rev. Quant. Nondestruct. Eval. 24 (2005) 385–392.
[19] T. Ulrich, P. Johnson, A. Sutin, Imaging nonlinear scatterers applying the time reversal mirror, J. Acoust. Soc. Am. 119 (2006) 1514–1518.
[20] P. Le Bas, K. Van Den Abeele, S. Dos Santos, T. Goursolle, O. Bou Matar, Experimental analysis for nonlinear time reversal imaging of damage materials, in: Proceedings of the European Conference on Non-Destructive Testing, Berlin, 2006.
[21] D. Cassereau, M. Fink, Time-reversal of ultrasonic fields – part 3: theory of the closed time-reversal cavity, IEEE Trans. Ultrason. Ferroelectr. 39 (1992) 579–592.
[22] A. Derode, P. Roux, M. Fink, Robust acoustic time reversal with high-order multiple scattering, Phys. Rev. Lett. 75 (1995) 4206–4209.
[23] G. Montaldo, P. Roux, A. Derode, C. Negreira, M. Fink, Generation of very high pressure pulses with 1-bit time reversal in a solid waveguide, J. Acoust. Soc. Am. 110 (2001) 2849–2857.
[24] P. Roux, B. Roman, M. Fink, Time-reversal in an ultrasonic waveguide, Appl. Phys. Lett. 70 (1997) 1811–1813.
[25] P. Roux, M. Fink, Time reversal in a waveguide: study of the temporal and spatial focusing, J. Acoust. Soc. Am. 107 (2000) 2418–2429.
[26] R. Ing, M. Fink, Time-reversed Lamb waves, IEEE Trans. Ultrason. Ferroelectr. 45 (1998) 1032–1043.
[27] C. Draeger, J. Aime, M. Fink, One-channel time-reversal in chaotic cavities: experimental results, J. Acoust. Soc. Am. 105 (1999) 618–625.
[28] C. Draeger, M. Fink, One-channel time-reversal in chaotic cavities: theoretical limits, J. Acoust. Soc. Am. 105 (1999) 611–617.
[29] C. Draeger, M. Fink, One-channel time-reversal of elastic waves in a chaotic 2D-silicon cavity, Phys. Rev. Lett. 79 (1997) 407–410.
[30] M. Fink, J. de Rosny, Time-reversed acoustics in random media and in chaotic cavities, Nonlinearity 15 (2002) R1–R18.
[31] J. Achenbach, Reciprocity in Elastodynamics, Cambridge University Press, 2003.
[32] E. Janssen, K. Van Den Abeele, Dual energy time reversed elastic wave propagation and nonlinear signal processing for localisation and depth-profiling of near-surface defects: a simulation study, Ultrasonics 51 (2011) 1036–1043.
[33] G. Montaldo, D. Palacio, M. Tanter, M. Fink, Time reversal kaleidoscope: a smart transducer for three-dimensional ultrasonic imaging, Appl. Phys. Lett. 84 (2004) 3879–3881.
[34] G. Montaldo, D. Palacio, M. Tanter, M. Fink, Building three-dimensional images using a time-reversal chaotic cavity, IEEE T. Ultrason. Ferroelectr. 52 (2005) 1489–1497.
[35] N. Quieffin, Etude du rayonnement acoustique de structures solides: vers un système d'imagerie haute résolution, Ph.D. thesis, Université Paris VI – Pierre et Marie CURIE, 2004.
[36] N. Quieffin, S. Catheline, R. Ing, M. Fink, Real-time focusing using an ultrasonic one channel time-reversal mirror coupled to a solid cavity, J. Acoust. Soc. Am. 115 (2004) 1955–1960.
[37] N. Quieffin, S. Catheline, R. Ing, M. Fink, 2D pseudo-array using an ultrasonic one channel time-reversal mirror, Ultrason. Symp. 1 (2004) 801–804.
[38] B. Van Damme, K. Van Den Abeele, Y. Li, O. Bou Matar, Time reversed acoustics techniques for elastic imaging in reverberant and nonreverberant media: an experimental study of the chaotic cavity transducer concept, J. Appl. Phys. 109 (2011) 104910.
[39] Y. Choi, H. Lee, H. Hong, W.-S. Ohm, Two-dimensional virtual array for ultrasonic nondestructive evaluation using a time-reversal chaotic cavity, J. Acoust. Soc. Am. 130 (5) (2011) 2720–2727.
[40] L. Fillinger, A. Sutin, A. Sarvazyan, Time reversal focusing of short pulses, Ultrason (2007) 220–223.
[41] O. Bou Matar, Y. Li, K. Van Den Abeele, On the use of a chaotic cavity transducer in nonlinear elastic imaging, Appl. Phys. Lett. 95 (2009) 141913.
[42] O. Bou Matar, Y. Li, S. Delrue, K. Van Den Abeele, Optimization of chaotic cavity transducers to nonlinear elastic imaging, in: Proceedings of the 10th French Congress on Acoustics, Lyon, 2010.
[43] B. Anderson, J. Douma, T. Ulrich, R. Snieder, Improving spatio-temporal focusing and source reconstruction through deconvolution, Wave Motion 52 (2015) 151–159.
[44] T. Ulrich, K. Van Den Abeele, P. Le Bas, M. Griffa, B. Anderson, R. Guyer, Three component time reversal: focusing vector components using a scalar source, J. Appl. Phys. 106 (2009) 113504.